



HAL
open science

Estimating the Probability Density Function of the Electromagnetic Susceptibility from a Small Sample of Equipment

Thomas Houret, Philippe Besnier, Stéphane Vauchamp, Philippe Pouliguen

► **To cite this version:**

Thomas Houret, Philippe Besnier, Stéphane Vauchamp, Philippe Pouliguen. Estimating the Probability Density Function of the Electromagnetic Susceptibility from a Small Sample of Equipment. Progress In Electromagnetics Research B, 2019, 83, pp.93 - 109. 10.2528/pierb18110703. hal-02052910

HAL Id: hal-02052910

<https://hal.science/hal-02052910v1>

Submitted on 4 Mar 2019

HAL is a multi-disciplinary open access archive for the deposit and dissemination of scientific research documents, whether they are published or not. The documents may come from teaching and research institutions in France or abroad, or from public or private research centers.

L'archive ouverte pluridisciplinaire **HAL**, est destinée au dépôt et à la diffusion de documents scientifiques de niveau recherche, publiés ou non, émanant des établissements d'enseignement et de recherche français ou étrangers, des laboratoires publics ou privés.

Estimating the Probability Density Function of the Electromagnetic Susceptibility from a Small Sample of Equipment

Thomas Houret^{1, 2}, Philippe Besnier¹, Stéphane Vauchamp² and Philippe Pouliguen³

Abstract—The failure risk of electronic equipment submitted to an electromagnetic aggression may be seen as the conditional probability that the susceptibility level of equipment is reached, knowing that a given constraint is applied. This paper focuses on the estimation of the probability density function of the susceptibility level of equipment. Indeed, the production variability of electric / electronic equipment under analysis implies that its susceptibility level may be considered as a random variable. Estimation of its distribution through susceptibility measurements of a limited set of available equipment is required. Either a Bayesian Inference (BI) or a Maximum Likelihood Inference (MLI) may be used for assessing the most probable density function. Above all, we highlight that they have to be used to delimit a set of probable distribution functions rather than the most probable one. It then provides realistic bounds of the failure probability at a given test level. First both types of inference are carried out on theoretical distributions. Then we compare the two methods on a virtual piece of equipment whose distribution is not known a priori but can be estimated a posteriori. Finally, we apply these inferences on a set of actual susceptibility measurements performed on several copies of equipment. We check that for extremely small sample size (a dozen) the Bayesian approach performs slightly better. However, above around 40, both methods perform similarly. In all cases, the likelihood estimations provide a clear statement of the probabilistic estimation of the statistics of susceptibility level given a limited sample of pieces of equipment.

Keywords: Electromagnetic compatibility, Risk analysis, Electromagnetic susceptibility, Failure probability inference.

1. INTRODUCTION

Failure risk assessment of electronic equipment to an electromagnetic aggression is the cornerstone of Intentional Electromagnetic Interference (IEMI). Evaluating the risk of failure of equipment is needed to set up electromagnetic protections. Pieces of electronic equipment are different from one another due to the fabrication tolerance of numerous components. As a result each piece of equipment may have a different susceptibility level. Knowing the behavior of the variations of susceptibility is useful for computing safety margins. Evaluating these variations is only possible from experiments. In the present framework, equipment is submitted to a conducted disturbance by a transient IEMI whose intensity is increased until a failure occurs. The susceptibility threshold is then denoted by the peak current induced on the equipment. From a set of measured susceptibility thresholds, the susceptibility probability distribution may be estimated. However, due to time and cost limitations, the set of available equipment for tests is limited to a few tens of units or less. The purpose of this paper is to identify the most probable probability density function (pdf) and the credibility intervals of its parameters as a function of the sample size.

The problem stated is in fact a classical problem of statistical inference: estimating unknown characteristics (underlying distribution function and its parameters) of a population (susceptibility

* Corresponding authors: Thomas Houret (thomas.houret@insa-rennes.fr), Philippe Besnier (philippe.besnier@insa-rennes.fr), Stéphane Vauchamp (stephane.vauchamp@cea.fr), Philippe Pouliguen (philippe.pouliguen@intradef.gouv.fr)

¹ INSA Rennes, CNRS, IETR UMR 6164, F-35000 Rennes, France. ² CEA DAM F-46000 Gramat, France. ³ DGA-MRIS F-75509, Paris, France

levels) from a limited set (susceptibility level measurements) of this population. The novelty of this paper does not concern the statistical inference itself. We only discuss and compare the choice of inference method, either from a frequentist or Bayesian point of view for small samples. The most important result for EMC analysis is that inference techniques induce that a single (even most probable distribution) distribution should not be used. A set of possible (credible) ones must be rather used to assess the probability of failure.

From a statistical point of view, assessing the susceptibility level of electronic equipment to IEMI is obviously a key for electromagnetic protection. Nitsch et. al. [1] have submitted a range of micro-controllers circuits and microprocessors to IEMI with various behaviors according to their inner technology. The random nature of cables or PCB tracks was addressed from a theoretical and statistical point of view in [2] and [3], but active components were not considered. However, a high-level prediction analysis was proposed in [4] that accounts for the electronic circuits topology. We may note also that [5] provides a general frame to perform a risk analysis, featuring a fault-tree analysis whose calculation requires knowledge of the distribution functions of involved parameters. From these publications (and others), it appears that an experimental approach is still relevant, but suffers from being limited to small numbers of entities. In a recent publication, Yuhao et. al proposed to use a Bayesian approach to estimate the susceptibility distribution from a limited set of experiments [6]. However, only a best estimate is provided. Our paper aims at reinforcing this method in analyzing the added value of a Bayesian approach and establishing the likelihood of the probability density and confidence intervals of relevant quantiles of the susceptibility level.

It is well known that Bayesian inference (BI) [7, 8, 9, 10, 11, 12] may be best suited for small sample size if a non-informative prior is used for the parameters of the probability density function. We aim at determining if a Bayesian inference is a critical tool to infer the susceptibility probability distribution with respect to the frequentist version of maximum likelihood inference (MLI) [13, 14, 15, 16]. In a previous communication [17], we studied the performance of different tests based on BI or MLI to select a hypothetic underlying distribution among a restricted set of functions (Normal, Lognormal or Weibull), before estimating their parameters. In this paper we provide a deeper view about the variance of these estimations as a function of the size sample. We first perform a Monte Carlo study to assess the variance of these estimators. Most importantly, once the parameter estimation is achieved, we determine credibility intervals for the parameters of the underlying distribution. As a result, a bundle of possible distributions is obtained which is likely to contain the true distribution. We highlight the performance of this approach using a virtual case as an example. We validate that the true distribution lies in the bundle for a series of Monte Carlo simulations. We then apply it to different sets of actual measurements. Eventually, we conclude that any quantile of the the probability of failure function may be bounded within an adequate interval, which is a key result for EMC risk analysis.

This paper is organized as follows. First, we briefly recall the principles of BI and MLI methods of inference (section 2). Then, we provide a Monte Carlo analysis of their relative performance as a function of the sample size (section 3). Section 4 is devoted to an EMC numerical example of a virtual simple printed circuit board (PCB) used to confirm the performance of the process. In section 5, we infer the likelihood of levels of susceptibility from several sets of tests of power supplies.

2. INFERENCE METHODS

In this section we briefly recall the MLI and BI principles. These two inference methods differ according to the estimation of the vector of parameters θ of the underlying assumed distribution function. For the distributions we deal with in this paper, the vector θ has two components, $\theta(1)$ and $\theta(2)$. When the distribution is Normal, $\theta(1)$ is the mean μ , and $\theta(2)$ is the variance σ^2 . When the distribution is Weibull, $\theta(1)$ is the scale γ , and $\theta(2)$ is the shape β .

As far as the MLI is concerned the vector of parameters to be estimated is deterministic, whereas for the BI it is a random variable. The result of the BI is therefore a probability distribution of the random vector of variables θ , whereas the result of the MLI is a likelihood function. However, since this likelihood function is expressed in terms of probabilities, it can also be interpreted as a probability distribution. Credibility intervals (for BI) or confidence intervals (for MLI) may therefore be computed in the same way for both inferences. There is no need to provide a prior distribution for the MLI. For

the BI, the user is free to choose an adequate prior . Performing MLI is equivalent to use a BI with a uniform distribution for θ .

2.1. Maximum likelihood inference

For each of the considered underlying, Normal (N), or Weibull (W) distribution, the vector of their two parameters is estimated from a frequentist point of view, using a maximum likelihood function. For the N case see [13, 14] and for the W case see [14].

2.2. Bayesian inference

According to Bayes theorem, the result of the BI is expressed as a density function called f_{post} of the estimated parameters:

$$f_{post}(\theta|Data) = \frac{f_{prior}(\theta)f_{like}(Data|\theta)}{\int_{\theta} f_{prior}(\theta)f_{like}(Data|\theta)d\theta} \quad (1)$$

f_{prior} is the a priori density. The likelihood function is f_{like} . A normalization operation is needed to obtain a density function.

The BI needs a prior distribution of the parameters to be estimated. It is therefore possible to benefit from knowledge learned from previous experiences. However, if no knowledge is available, the non-informative prior has to be selected. In order to find such priors, two requirements must be followed. The first one is the maximal entropy and the second one is the parameter space scale invariance [7, 8]. The prior choice depends on the target distribution and on the method used to find it. There are three classical methods to obtain non informative priors:

- The Maximal Data information Prior (MDIP) of Zellner [9] which is based on the maximization of an information criterion
- The Jeffrey's prior which is based on the Fisher information matrix [10].
- The so-called Reference prior [11] which is a modification of the Jeffrey's prior.

For a targeted distribution, more than one prior is possible. But different methods can lead to the same prior. There is a catalog of priors for popular distributions including N and W ones [12]. We used the MDIP for the N distribution (which is the same as the Reference prior):

$$f_{prior}(\mu, \sigma^2) = \frac{1}{\sigma^2} \quad (2)$$

And, the Jeffrey's prior is used for the W distribution (which is also the same as the reference prior):

$$f_{prior}(\gamma, \beta) = \frac{1}{\gamma \cdot \beta} \quad (3)$$

The prior choice becomes less important as the sample size increases. For a large enough sample size the prior choice does not affect the posterior distribution. Furthermore, using a uniform distribution, the BI is equivalent to the MLI. In the frame of susceptibility level evaluation, the likelihood function is written:

$$f_{like}(Data|\theta) = \prod_{e=1}^n \Psi(st_e, \theta) - \Psi(st_e - \delta, \theta) \quad (4)$$

The function Ψ is the cumulated distribution function (cdf) of the distribution. If true distribution is N:

$$\Psi(s, \mu, \sigma) = \frac{1}{2} \left(1 + \operatorname{erf} \left(\frac{s - \mu}{\sigma \sqrt{2}} \right) \right) \quad (5)$$

If true distribution is W:

$$\Psi(s, \gamma, \beta) = 1 - e^{-\left(\frac{s}{\beta}\right)^\gamma} \quad (6)$$

The δ variable is the step precision of the levels of the peak current applied during the susceptibility test. Furthermore, st_e is the level of peak current that provoked a failure of the e^{th} equipment whereas the constraint $st_e - \delta$ had no effect. Once the susceptibility threshold is reached the equipment is supposed to remain in failure for higher test levels and the test stops at st_e level.

The inferences are based on the underlying distribution (whose cdf is Ψ). We addressed the problem of selecting the adequate distribution in [7]. In this paper, we focus on the parameter estimations resulting from the inference process, i.e. the estimation of θ and related quantities such as failure probability and susceptibility thresholds.

Both inferences methods provide a distribution (f_{post}) of the estimated parameter θ . The failure probability $p_f(s)$ which is defined as the probability to have a failure if the test level reaches the value of s is a more relevant information for EMC experts. Once the θ parameters are estimated, p_f can be induced from:

$$p_f(s) = \Psi(s, \theta) \quad (7)$$

However, θ is distributed according to the multivariate function f_{post} . Each couple of parameters ($\theta(1), \theta(2)$) has a likelihood proportioned to f_{post} evaluated at $(\theta(1), \theta(2))$. Therefore, at a level s , $p_f(s)$ follows itself a distribution of possible values.

As a consequence, $p_f(s)$ is associated with a beam of likely cdf plots. It is possible to bound this beam between an upper $U(s)$ and lower limit $L(s)$ with a confidence interval (here arbitrarily chosen at 95%). The bounds are the quantiles of $p_f(s)$ computed at every s . As a result:

$$\mathbb{P}\{p_f(s) \in [L(s), U(s)]\} \quad (8)$$

Beyond examination of p_f , EMC engineers may be more interested in a related quantity, the quantile s_α . This quantity corresponds to the test level at which a failure probability of α is reached.

Because the estimated θ is a distribution, s_α follows a distribution. It is convenient to induce a confidence interval $[s_{low}, s_{upp}]$ for s_α .

To compute such interval, we estimate the upper $U(s)$ and lower $L(s)$ bound of $p_f(s)$ for all s , at the confidence level of 95%. Then:

$$\begin{cases} s_{low} = U^{-1}(\alpha) \\ s_{upp} = L^{-1}(\alpha) \end{cases} \quad (9)$$

From the point of view of EMC susceptibility testing, and in the context of failure probability estimation of a piece of equipment under an uncertain constraint, the lower tail of the susceptibility distribution is particularly important. Indeed, under such scenario, the estimated probability distribution of the IEMI is analyzed in relation with the estimated probability distribution of the susceptibility. In many practical scenarios, only the upper tail of the constraint and the lower tail of the susceptibility overlap and determine the overall failure probability. That is why we examine the quality of the estimation of the susceptibility threshold in this region. We choose $\alpha=5\%$ as an example for the rest of the paper.

In order to evaluate the various estimators discussed, as a function of the sample size, Monte Carlo simulations are carried out.

We use 1000 Monte Carlo simulations, for each considered sample size. The detailed procedure for each of Monte Carlo trial is the following:

- (i) Generate a sample from the true distribution.
- (ii) Apply both inferences to compute the distribution of the estimated θ
- (iii) Localize the summit of the distribution (most probable realization) to have a scalar estimation of θ .
- (iv) Compute the distribution of s_α from the distribution of θ .
- (v) Deduce an interval containing the true s_α at a confidence level (here 95%)
- (vi) Store the quantities computed (the maximum likelihood distribution of f_{post} , bounds s_{low} and s_{upp}) for mean and variance analysis.

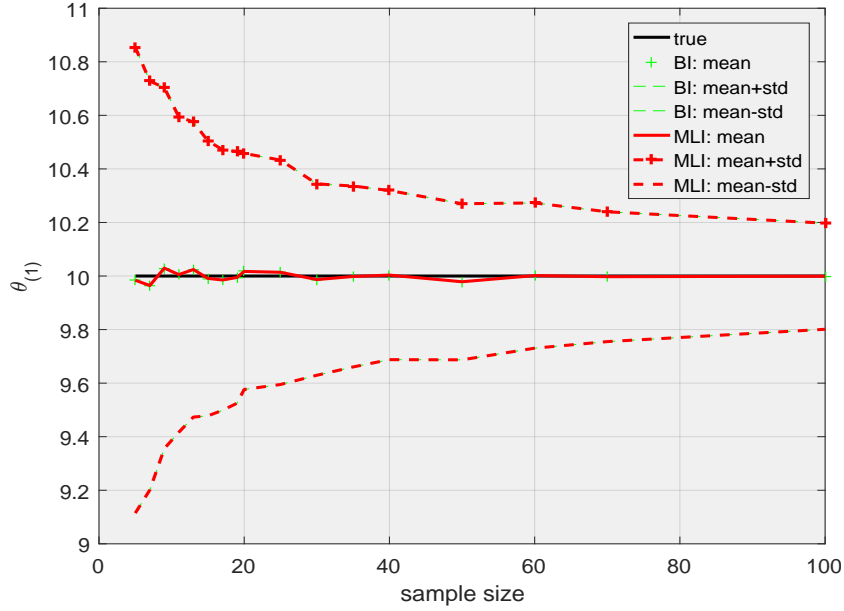


Figure 1. Estimation of the $\theta(1)$ parameter of a normal distribution as a function of sample size. Both BI and MLI lead to the same estimator.

3. THEORETICAL COMPARISON BI/MLI

In this section we compare the two methods of inference when the true distribution is Normal or Weibull. The true parameters of the underlying distribution are fixed such that the coefficient of variation (standard deviation over mean) is equal to 20%. In this section we suppose the two inferences use the right hypothesis (Normal in section 3.1 and Weibull in section 3.2.) First we compare the estimation of the two scalar components of θ . Then we compare the bounds of s_α .

3.1. Normal distribution

3.1.1. Parameters estimators quality comparison

From Monte Carlo simulation we compare the most probable values of $\theta(1)$ in Fig. 1 and $\theta(2)$ in Fig. 2 given by the inferences. More precisely, we compare their mean and variance.

The spread given by MLI and BI estimators of $\theta(1)$ are exactly the same because the marginal prior distribution of the first component ($\theta(1)$) is uniform. Therefore the choice of the inference does not matter for estimating the most probable $\theta(1)$.

In Fig. 2, the mean with BI is systematically smaller than the mean obtained from MLI. Both of them are smaller than the true value. The standard deviation with BI is slightly smaller than with MLI. Therefore the estimation is slightly more precise, especially for small n , with BI. BI leads to more bias but lower variance, whereas MLI leads to less bias but higher variance.

3.1.2. Bounding the susceptibility threshold s_α corresponding to a failure probability α

In Fig. 3 we plot the bounds of s_α with error bars indicating their standard deviation from BI and MLI (the length of one bar is equal to two times the standard deviation of the computed bound).

For large sample sizes, both inferences lead to similar bounds. Moreover, the benefit of getting a larger sample, beyond $n = 40$, is low as much larger increase of n is necessary to get significantly narrower bounds.

For small samples, the difference between the two inferences are more important for the lower bound. The minimum (mean minus standard deviation) of the BI lower bound is systematically closer to the true value minimum. For the upper bound, it is the contrary.

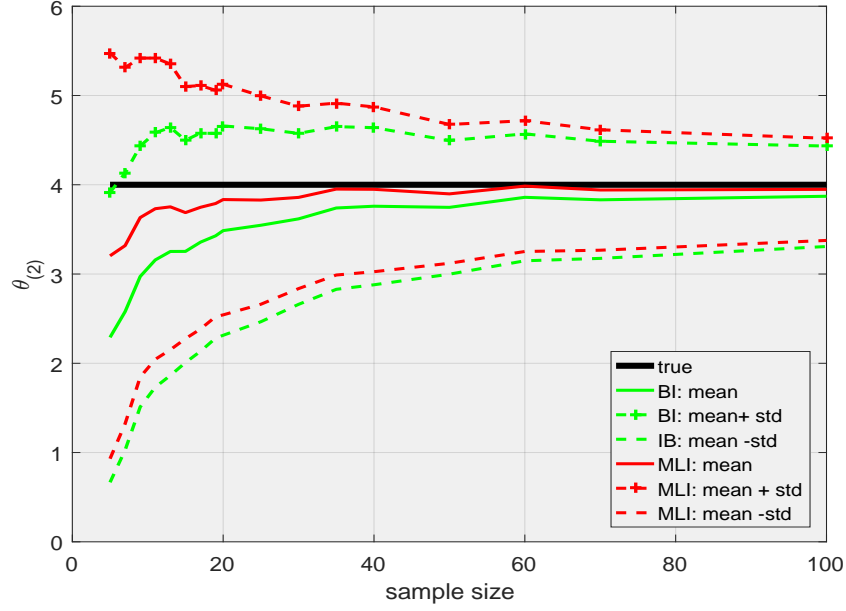


Figure 2. Estimation of the $\theta(2)$ parameter of a normal distribution as a function of sample size.

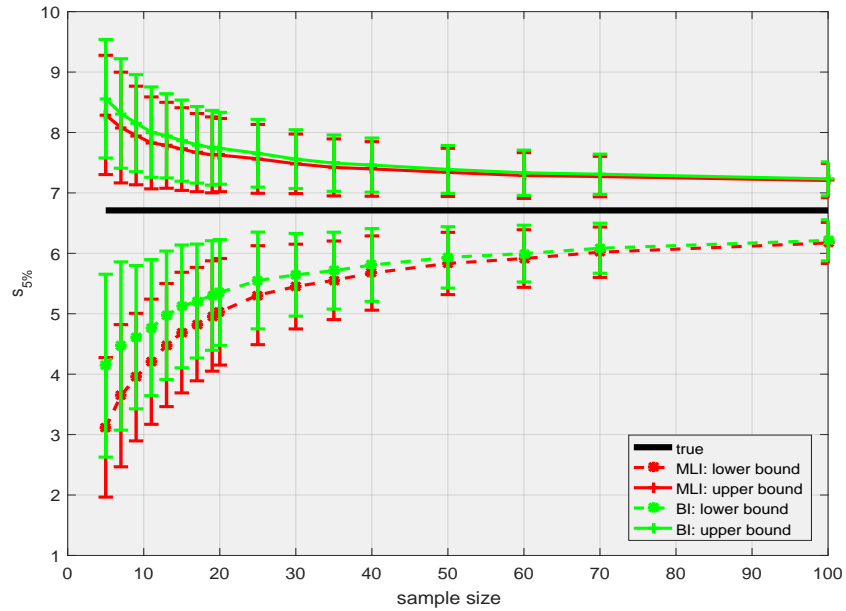


Figure 3. Estimation of the 5% quantile when the susceptibility distribution is Normal with parameter $\theta=[10,4]$. Errors bars length of two times the standard deviation.

As a result, BI performs better because the bounds are slightly narrower thanks to the lower bound.

3.2. Weibull distribution

We proceed here to the same analysis, but with a Weibull distribution.

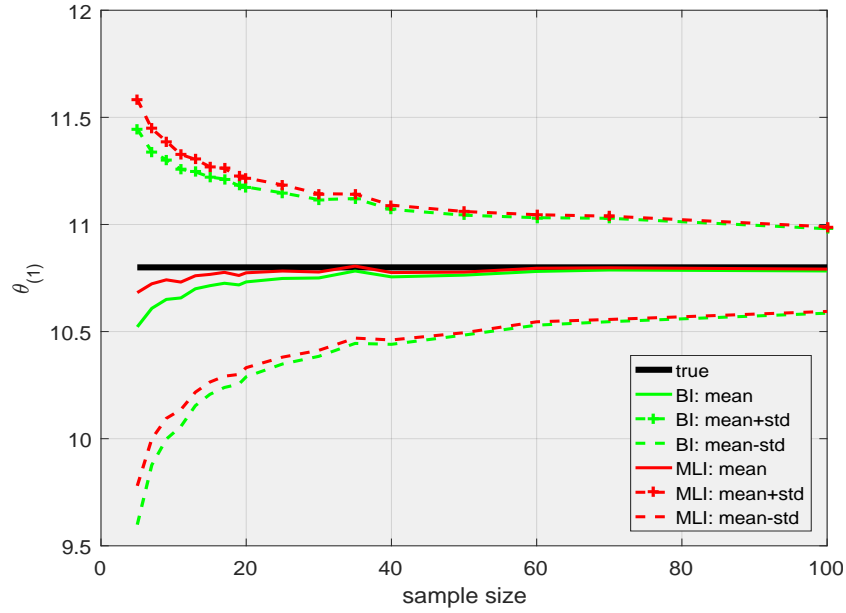


Figure 4. Estimation of the $\theta(1)$ parameter of a Weibull distribution.

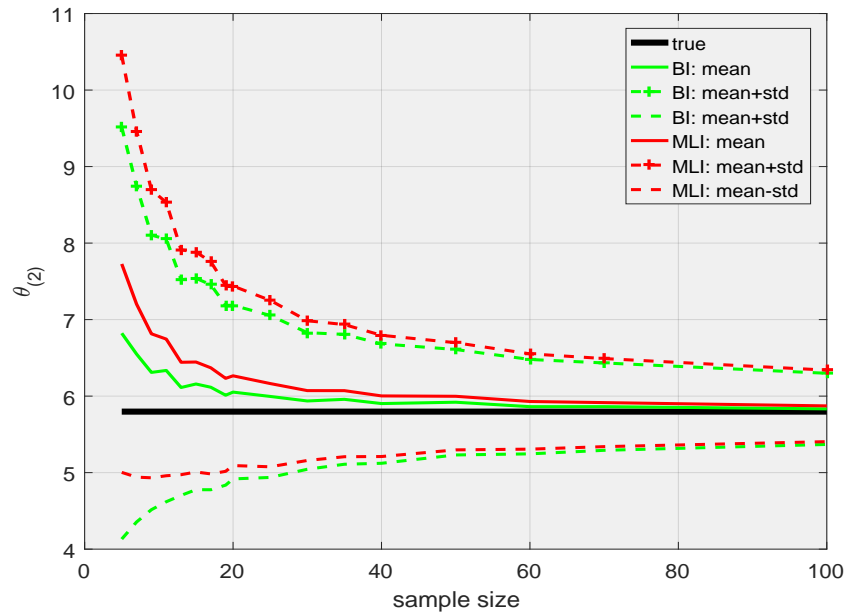


Figure 5. Estimation of the $\theta(2)$ parameter of a Weibull distribution.

3.2.1. Parameters estimators quality comparison

In Fig. 4, the mean estimator of $\theta(1)$ from MLI is slightly closer to the true value than the BI estimator. The standard deviations are similar. Therefore MLI is more relevant than the BI to estimate $\theta(1)$.

It is the contrary for the estimator of $\theta(2)$ in Fig. 5, since BI outperforms MLI (the mean of estimation of $\theta(2)$, is closer to the true value, with a similar standard deviation).

3.2.2. Bounding the susceptibility threshold s_α corresponding to a failure probability α

In Fig. 6, we plot the bounds of the susceptibility with error bars (the length of one bar is equal to two times the standard deviation of the computed bound) from BI and MLI.

For the Weibull distribution, the MLI performs better for the same reasons BI performed better in the Normal case.

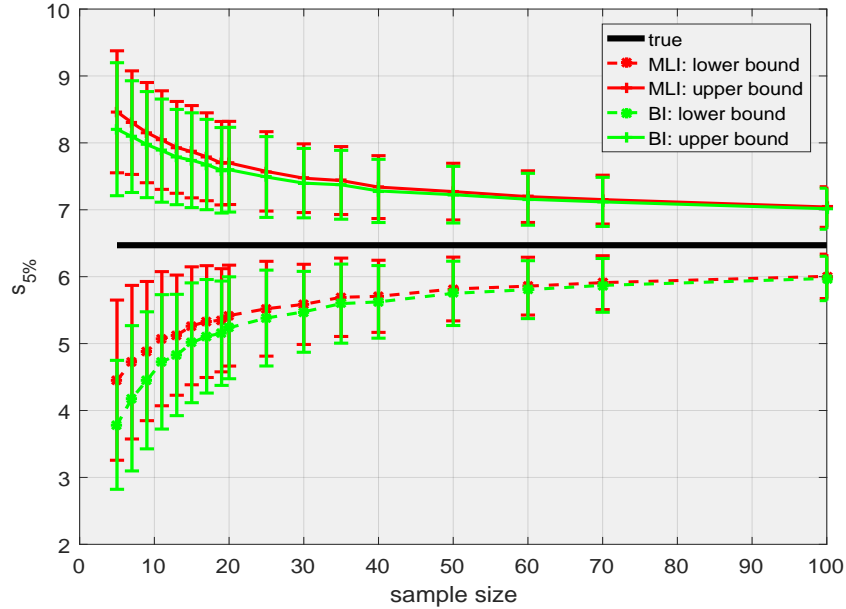


Figure 6. Estimation of the 5% quantile when the susceptibility distribution is Weibull with parameter $\theta=[10.80,5.80]$. Errors bars length of two times the standard deviation.

3.3. Consistency of credibility intervals of probability of failure distributions and confidence intervals of s_α

In the previous simulation, the likelihood of parameter estimations was used to retrieve confidence interval for the pdf of the susceptibility threshold and then for a quantile of the probability of failure. In the previous section only the mean and standard deviation of the confidence interval bounds were plotted. These bounds are computed according a single random set. Therefore the bounds are also random. As an example of the randomness of the bounds, we generated 5 sets of small size ($n=5$) from the above considered normal distribution and plotted the corresponding 5 upper and lower bounds in Fig. 7.

As the bounds are computed with a confidence interval of 95%, we expect that the threshold corresponding to a probability of failure of α is inside the interval defined by the lower and upper bound 95% of the time. The aim of this section is to check if this expectation is verified for an arbitrary chosen value $\alpha = 5\%$ with two different sample sizes.

To do so, we provide the distribution of the bounds from 1000 samples. The bounds distribution for the Normal distribution is plotted in Fig. 8 ($n = 5$), Fig. 9 ($n=100$) and for the Weibull distribution in Fig. 10 ($n = 5$), Fig. 11 ($n=100$). In Fig. 8, the MLI lower bound 97.5% quantile is much lower than $s_{5\%}$, whereas for BI we obtain the expected result. For the upper bound the BI and MLI bound 2.5% quantiles are close to $s_{5\%}$. As a result the MLI bound tends to be too conservative whereas BI is more optimal. In Fig. 10, the BI lower bound 97.5% quantile is lower than the true $s_{5\%}$ whereas the MLI quantile is close to it. Both upper bounds 2.5% quantile are slightly too low. As a result the BI bound is too conservative whereas MLI is more optimal.

The difference between the expectation and the observations might come from the bias of the estimators of the distribution parameters. With the $n = 100$ sample size, we notice, in Fig. 9 and 11,

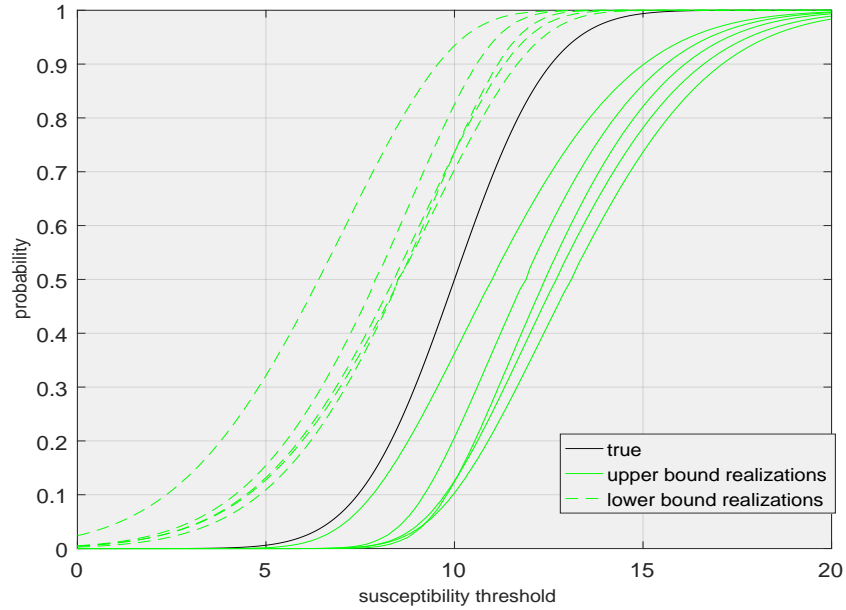


Figure 7. Example of a few bound realizations of the true susceptibility probability computed from 5 sets of small size ($n=5$).

that both inference bounds are similar and that the 2.5% and 97.5% quantiles are very close to the true value of $s_{5\%}$.

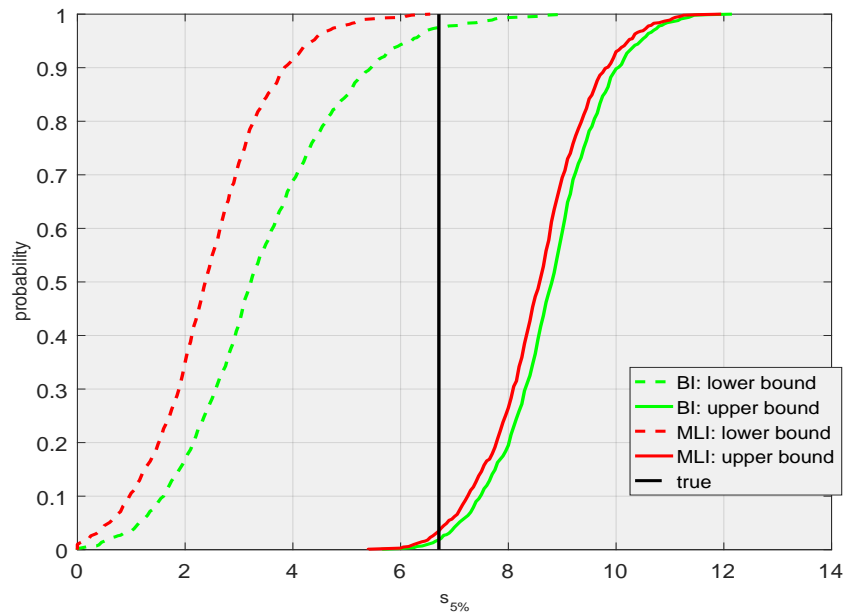


Figure 8. Distribution of the bounds of the 5% quantile computed from a small sample ($n=5$) from a Normal distribution with parameter $\theta=[10,4]$.

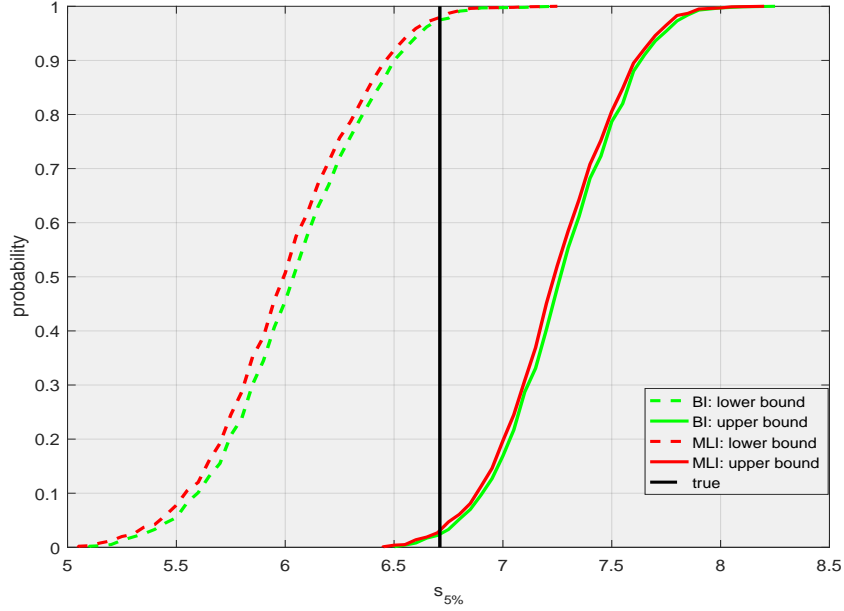


Figure 9. Distribution of the bounds of the 5% quantile computed from a large sample (n=100) from a Normal distribution with parameter $\theta=[10,4]$.

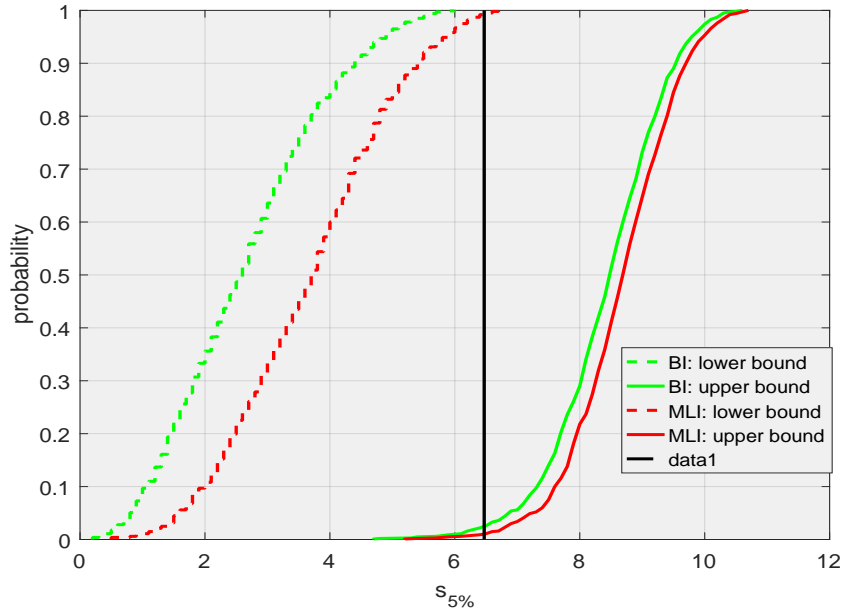


Figure 10. Distribution of the bounds of the 5% quantile computed from a small sample (n=5) from a Weibull distribution with parameter $\theta=[10.80,5.80]$.

4. APPLICATION ON A VIRTUAL EQUIPMENT

4.1. Utility of a virtual application

The virtual case example corresponds to random generation of susceptibility thresholds obtained from electromagnetic simulation of electronic equipment. It is an intermediate case between the theoretical simulations (true distribution known a priori) performed in section 3 and a real case with susceptibility measurements in section 5 (true distribution forever unknown unless very large sample is available). A

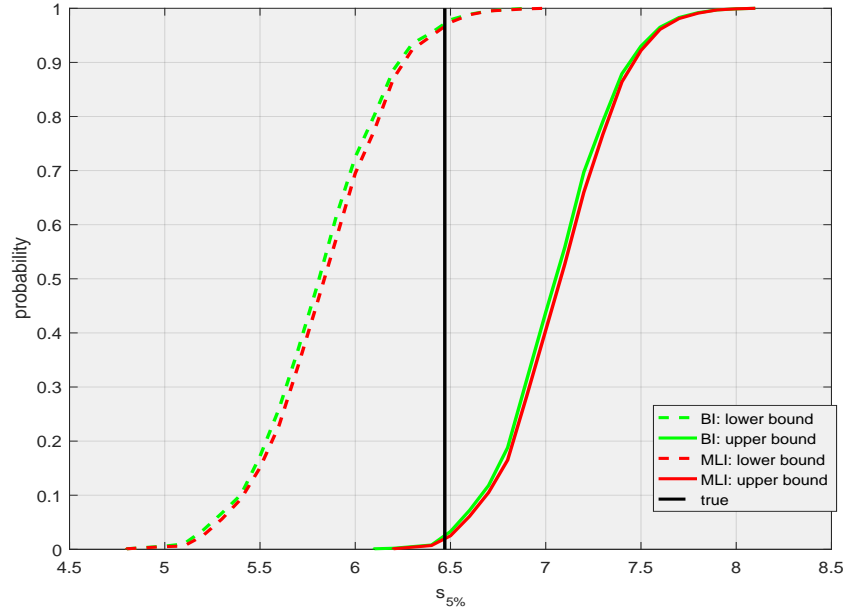


Figure 11. Distribution of the bounds of the 5% quantile computed from a large sample ($n=100$) from a Weibull distribution with parameter $\theta=[10.80, 5.80]$.

pseudo-reference in the virtual equipment case can be retrieved. Indeed, much more copies of equipment can be simulated than it would be possible to test in practice. Moreover, in the theoretical section, the true nature of the distribution (normal or Weibull) was known before applying the inferences. This knowledge is often not available in practice. Therefore in the virtual equipment case, the BIC criterion is used before the inferences. The BIC criterion will decide which amongst three distributions (Normal, Weibull, Lognormal) the sample is more likely to be sampled from.

This example has been chosen to be simple enough to perform simulations within an acceptable time (43 seconds per HFSS simulation). This large sample size allows us to obtain an empirical estimation of the distribution and may be considered as a pseudo-reference for smaller sample sizes retrieved from the large sample. Both BI and MLI inferences are tested on these smaller samples. We consider this example as a modeling application since it is made of an electronic equipment (even if it is simple and arbitrary) and most of all, the variability of the susceptibility threshold is generated by variation of physical parameters.

4.2. Equipment design

We designed a simple electronic piece of equipment presented in Fig. 12. The considered piece of equipment is a printed circuit board with two microstrip lines $L1$ and $L2$. The microstrip line $L1$ is ended by matched resistive loads. The microstrip line $L2$ is ended at one end by a resistor and at the other one by a transistor. Whereas $L2$ is entirely covered by a grounded shield whereas $L1$ is partially covered. A small aperture is made at the shield interface so that the microstrip line gets out of the shielded box. The uncovered portion of $L1$ is illuminated by an electromagnetic continuous plane wave, at 500 MHz, with normal incidence and polarized in the parallel direction to the uncovered portion of the line $L1$. Underneath the shielding, $L1$ and $L2$ are close to one another which cause a crosstalk coupling. The nominal dimensions of the design are: $L1 = 205$ mm, $L2 = 130$ mm, the ground plane has an area of 250 mm \times 250 mm and the FR4 substrate thickness is 1.7 mm.

The variability of the susceptibility is ensured by the randomness of multiple parameters (lines length, loads, parasitic capacitor of the transistor [18]) around the design nominal value (variability arbitrary set to 10%). Therefore, each device is a random realization.

The field intensity is (virtually) raised until provoking a failure. The failure criterion is associated to the output (Vds) of a transistor mounted as an inverter. When no constraint is applied, the input

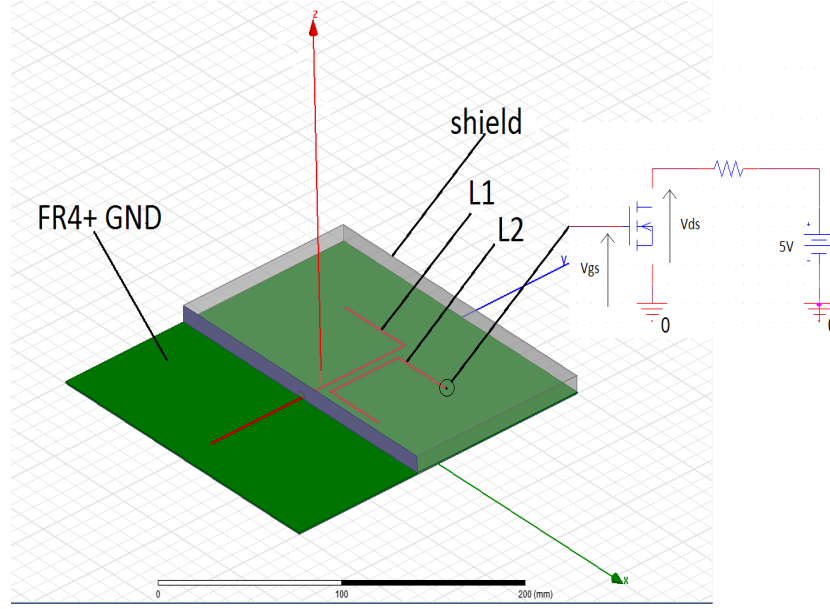


Figure 12. Virtual equipment

voltage (V_{gs}) is at 0 V and therefore the output (V_{ds}) is at 5 V. The transistor is blocked. If is lower than an arbitrary threshold V_{th} , the transistor is supposed to be out of a prescribed tolerance and this is considered as equipment failure.

The empirical pdf is obtained from a simulation of $n_c=2000$ random copies of that equipment. We call that set the reference sample. The number n_c was chosen to be much larger than samples of size n of interest (a few tens) but not too large to be compatible with reasonable simulation times (about 23 hours). With $V_{th}=4$ V, the n_c simulated thresholds are represented in Fig. 13. The choice of V_{th} only translates (and preserves the shape) the thresholds distribution to higher levels if V_{th} decreases for example. The complete sample of threshold data is plotted in Fig. 13 as well as the best possible fit according to three distributions (Normal, Lognormal and Weibull). The fit are based on the scalar MLI estimation of θ .

Like in practical measurements neither the true distribution Ψ nor the true value of s_α are known. Thanks to the simulation capability, the true s_α can be estimated from the complete sample. Then we estimate the bounds of s_α for a sample of size n ($5 \leq n \leq 100$). For each sample the distribution function Ψ is chosen from a restricted set of possible distribution (Normal, Lognormal and Weibull) according to the BIC criterion [17]. The Ψ distribution can be either Normal, Weibull or Lognormal depending on the choice made at each sample (Normal or Weibull are more likely to be chosen). The same Ψ function is used when applying BI or MLI for computing the bounds. The estimation spread of s_α is computed as described in section 3 using the cdf of the distribution selected by the BIC.

4.3. Results

Results are provided in Fig. 14. The bounds, calculated at 95% confidence interval, converge slowly to the pseudo-reference. The two methods of inferences have very similar performance, for the upper bound and for the lower bound beyond $n=30$. For very small sample size, the mean of the lower BI lower bound is closer to the reference. The minimum (mean minus standard deviation for the lower bound) is almost identical for the two inferences. For extremely small sizes, the mean plus standard deviation is closer to the reference in case of BI lower bound. As a result there is a small advantage in favor of the BI thanks to the lower bound.

In Fig 15 and in Fig. 16 we plot the distribution of the bounds of $s_{5\%}$ for a small sample size ($n = 5$) and a large one ($n = 100$), respectively. Unlike the theoretical cases, the true distribution is not available. A best possible fit of the the reference sample against possible distributions was performed

in Fig. 13. From the complete reference sample three $s_{5\%}$ quantiles were computed. One empirical, one from the normal best fit, and one from the Weibull best fit. It is not possible to decide which of this three quantiles has to be considered as the true quantile because each is in fact an estimation of the true quantile.

As the true $s_{5\%}$ is unknown it is difficult to rigorously assess the performance of bounds estimation. Nevertheless some interesting observation can be made. For the small sample, the lower/upper bounds from both inferences are very similar. For the lower bound, the MLI 97.5% quantile appears to be closer to the true $s_{5\%}$ than the the BI 97.5% quantile. For the large sample size, the distributions of the bounds of both inferences merge together. For the upper bounds the 2.5% quantile is close to the normal best fit quantile whereas the lower bounds 97.5% quantile is close to the empirical quantile. This highlight the effect of choosing the true distribution nature when applying the inference. Therefore, the targeted confidence interval probability is not be exactly observed (error of about 5%) due to the distribution selection in the case of the virtual equipment. Netherville, we conclude that the confidence interval of s_α almost certainly includes the true value of s_α .

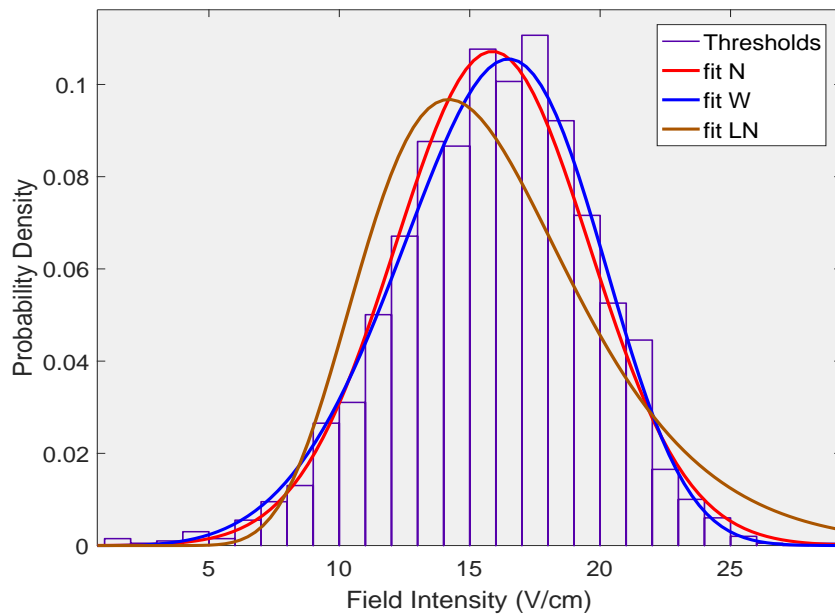


Figure 13. Reference susceptibility distribution

The procedure is now applied to analyze a series of tests on actual equipment.

5. APPLICATION TO ACTUAL MEASUREMENTS

In the framework of the susceptibility studies on electronic equipment, the french C.E.A. (Commissariat à l'énergie atomique et aux énergies alternatives) in Gramat, measured the susceptibility of two families of AC/DC power supplies against currents injections. The thresholds presented in this paper have been normalized for disclosure. Moreover, neither reference is available for the tested equipment, nor previous knowledge on the susceptibility distribution. This application case would be the most common scenario in practice.

In Table. 1 we present for each family the susceptibility measurements. The families are arbitrary named A and B with a sample size of respectively 12 and 20. The last test level applied provoked a failure of the equipment. As it is the case in real life, the susceptibility level was quantified (step level). The test levels at which it was possible to stress the equipment are reported on the last column.

In Table. 2 we present the result of the analysis of the measurement. The BIC criterion is used to choose a distribution type. The estimated parameter θ (the most probable one) is reported as well as the chosen hypothesis for each family. Finally in the last column we present the bounds of s_α thanks to the procedure described in this paper.

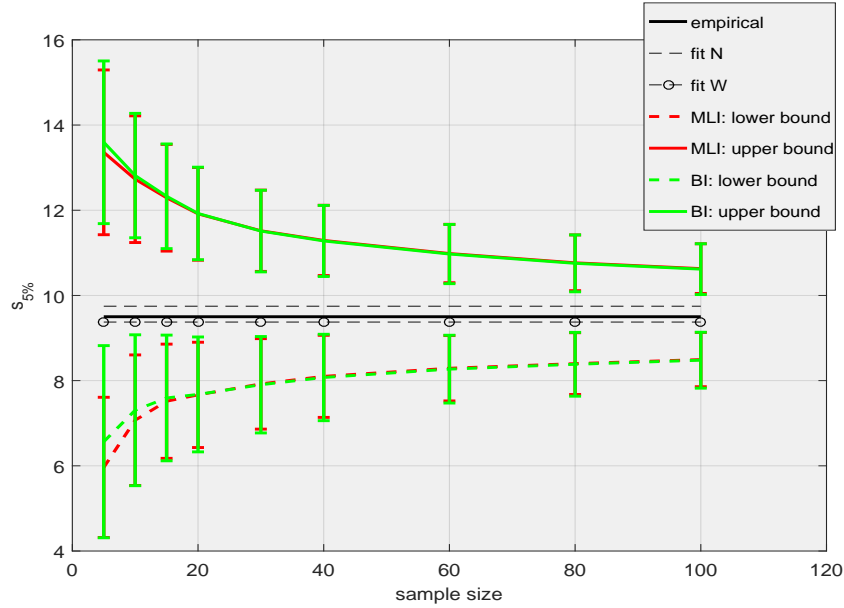


Figure 14. Application case. bounding the true $s_{5\%}$ (complete sample: empirical quantile, weibull fit and normal fit) from sub-samples of the complete sample. Errors bars length of two times the standard deviation.

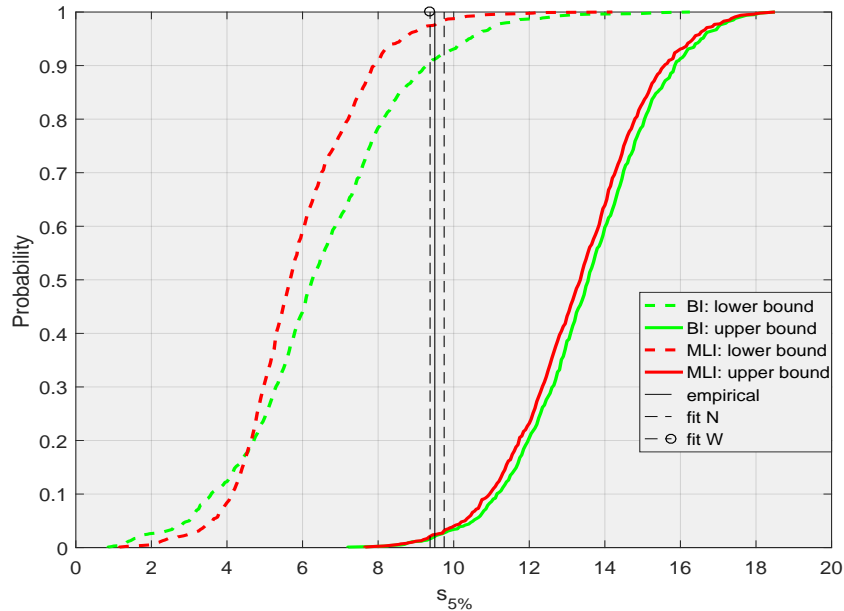


Figure 15. Application case. Distribution of the bounds of the true 5% from a small sub-sample ($n = 5$).

In the Fig. 17 and Fig. 18 we plot the result for the empirical cdf, the most probable cdf and the bounds of p_f at confidence level of 95% at every susceptibility level. The most probable cdf is obtained by selecting only the most probable θ (i.e. the maximum of $f_{post}(\theta)$). The BI bounds are slightly narrower with the BI thanks to the upper bound. This is more significant with the family A than with the B one.

In Fig. 19 and Fig. 20 we plot a view of the posterior distribution of the estimated θ , as multiple isoprobabilistic contours. Hotter colors lines indicate higher probabilities. The spread of parameters

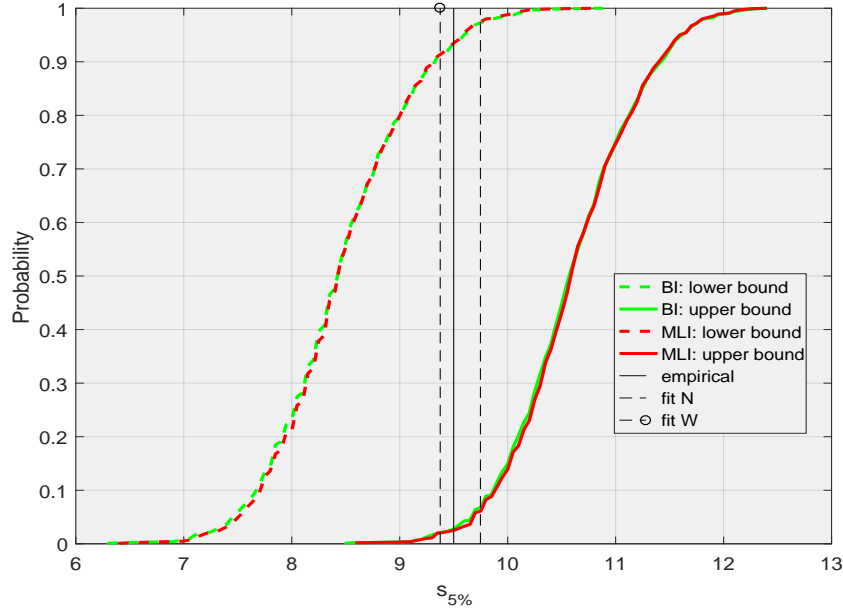


Figure 16. Application case. Distribution of the bounds of the true 5% from a large sub-sample ($n = 100$).

Table 1. Susceptibility measurements

Families	Failure levels (Amperes)	Constraint levels (Amperes)
A	[5.6,5.6,7.3,8.9,8.9,8.9,8.9,8.9,16.9,10.5,10.5,13.7]	[2.4, 4, 5.6, 7.3, 8.9, 10.5, 12.1, 13.7, 16.9]
B	[3.9, 6.3, 9, 14.7, 9, 6.3, 3.9, 9, 14.7, 3.9, 14.7, 6.3, 3.3, 9, 12.1, 3.9, 12.1, 3.9, 12.1, 21.4, 3.9]	[1.8, 3.9, 6.3, 9, 12.1, 14.7, 17.9, 21.4]

Table 2. Susceptibility measurements analysis

Families	Chosen hypothesis from BIC	$\theta(1),\theta(2)$	MLI bounds of $s_{5\%}$	BI bounds of $s_{5\%}$
A	Log Normal	2.21 0.29	[2.95 , 6.52]	[3.49, 6.69]
B	Log Normal	2.06 0.24	[1.85 , 4.30]	[2.03, 4.42]

estimations in Fig. 19 and Fig. 20 explains the bounds of pdf Fig. 17 and Fig. 18 respectively.

6. CONCLUSION

This paper is dedicated to the statistical inference of the susceptibility distribution of electronic equipment when the number of equipment available for test is small. The goal was to determine which approach, the BI or the MLI, was best suited in that case and to extract credibility or confidence intervals for the probability of failure.

We used a Monte Carlo simulation to compare the distribution of the bounds of the 5% failure probability which is a key parameter for EMC risk analysis in the frame of IEMI.

The comparison was made on three cases. The three cases are in ascending uncertainty with regard to the true distribution. In the first case (theoretical distribution) the true distribution is known a priori, in the second (virtual equipment) it is estimated and in the last (measurements) it cannot be

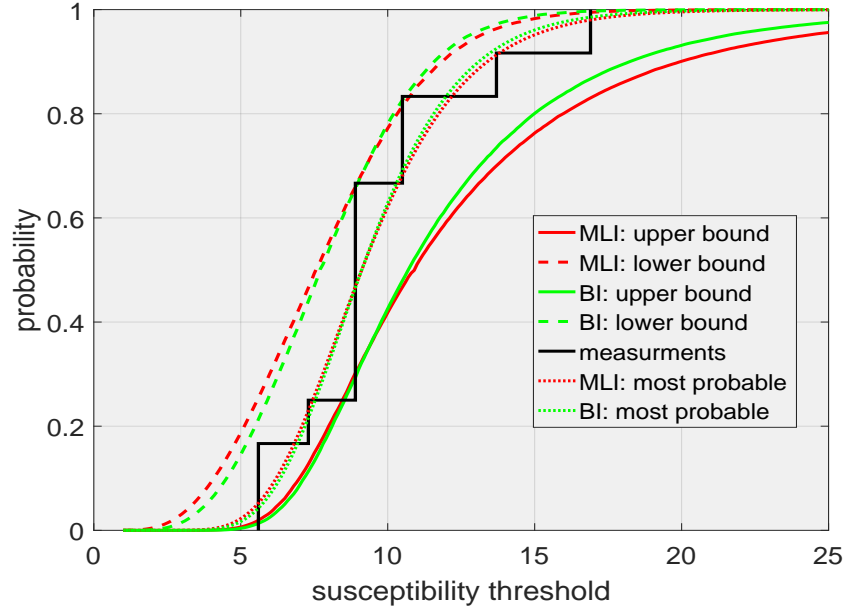


Figure 17. Family A estimated susceptibility thresholds distribution: empirical (black), most probable (from BI) (green small dot) and from MLI (red small dot) and bounds of confidence: upper bound with BI (green dot) , with MLI (red dot) and lower bound with BI (green), with MLI (red).

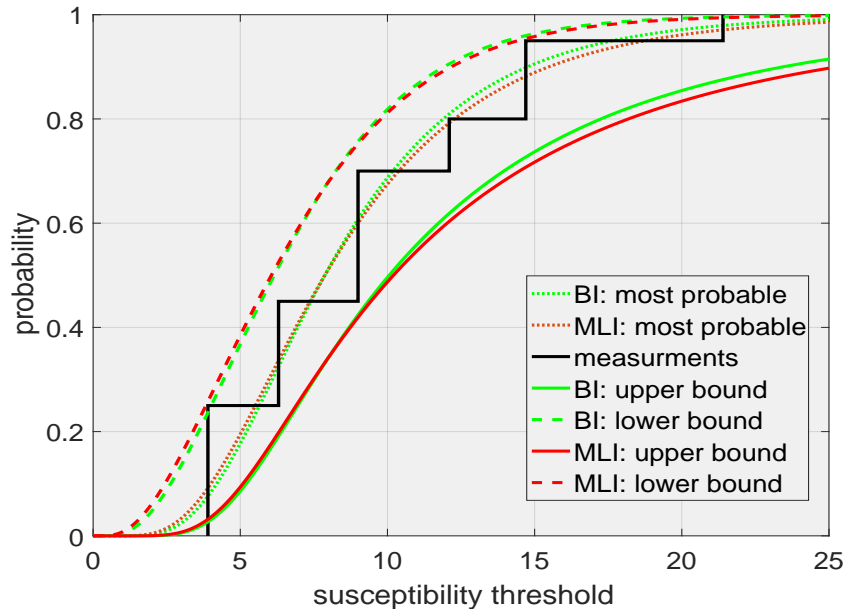


Figure 18. Family B estimated susceptibility thresholds distribution.

determined.

Our study showed that both methods become identical for sample size larger than 40. Therefore, we recommend for medium and large samples (> 40), to use MLI or BI indifferently. For small samples (< 40), we found that BI is better for Normal distributions but MLI is better for Weibull distributions. In the virtual equipment case, the susceptibility distribution could be Normal or Weibull. In that case, the BI is slightly better. Therefore, we recommend for very small sample to consider the BI as a relevant inference tool.

The main available feature of MLI or BI which is shown in this paper to be relevant for EMC risk

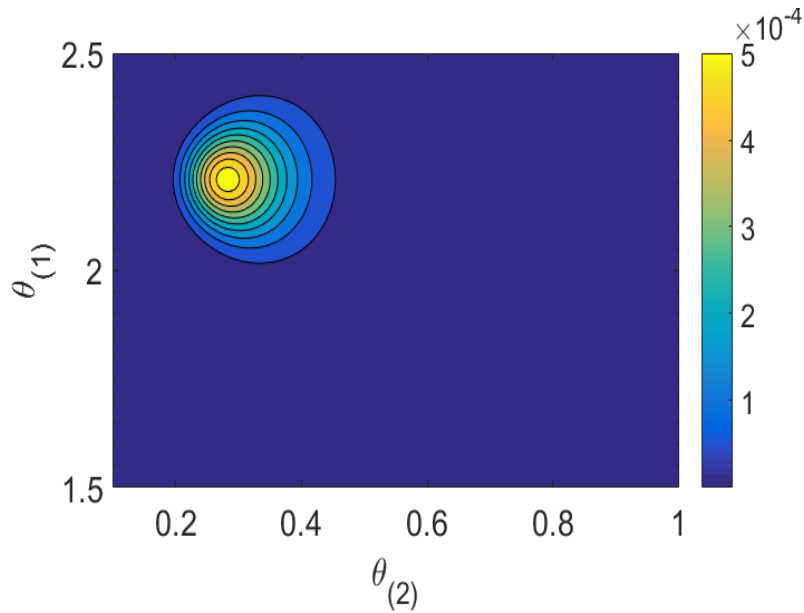


Figure 19. View of $f_{post}(\theta)$ contours for A family (BI only).

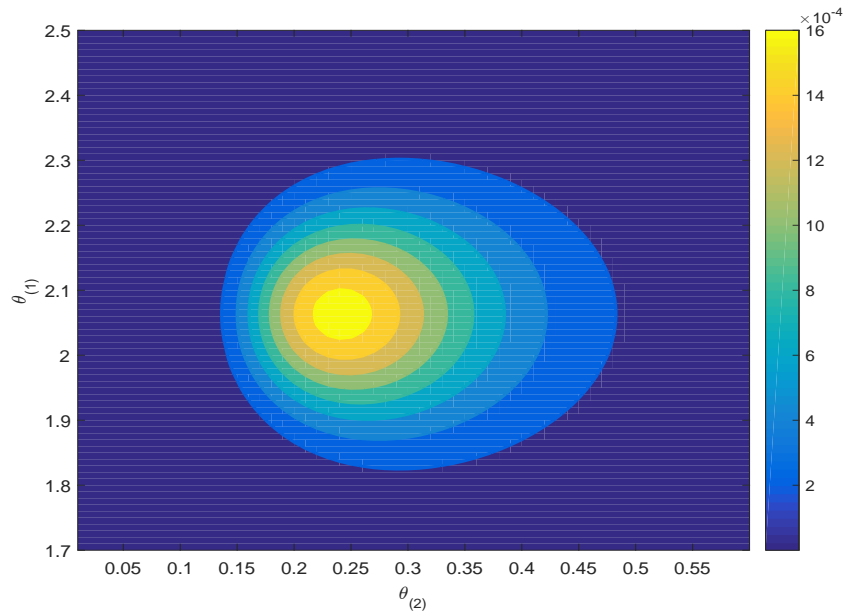


Figure 20. View of $f_{post}(\theta)$ contours for B family (BI only).

analysis is that they enable to find a range of possible values for the distribution parameters. Using this range of values, a set of possible distribution functions may be found from a single sample of recorded susceptibility levels from several pieces of equipment. In turn a confidence interval may be found for a quantile of the probability of failure. This confidence interval may be large but bounded including for a very small sample size. However, reduced confidence intervals are reached if the size reaches a dozen. Besides the choice of inference method it is important not to settle for a most probable estimation at the risk of forgetting the large uncertainty due to the small sample size. A more relevant approach for EMC risk analysis is therefore to use the credibility intervals of the parameter estimations and associated confidence intervals for the probability of failure.

ACKNOWLEDGMENT

The authors would like to acknowledge the support from the D.G.A. (Direction Générale de l'Armement).

REFERENCES

1. Nitsch, D., Camp, C., Sabath, F., "Susceptibility of some electronic equipment to HPEM threat," *IEEE Trans. Electromagn. Compat.*, Vol. 46, No. 3, 2014.
2. Spadacini, G., Pignari, S.A. "Numerical assessment of radiated susceptibility," *IEEE Trans. Electromagn. Compat.*, Vol. 55, No. 5, 956–964, 2014.
3. Mehri, M., Masoumi, N., Rashed-Mohassel, J., "Trace orientation function for statistical prediction of PCB radiated susceptibility and emission," *IEEE Trans. Electromagn. Compat.*, Vol. 57, No. 5, 1168-1178, 2015.
4. Mehri, M., Masoumi, N., Rashed-Mohassel, J., "Statistical prediction and quantification of radiated susceptibility for electronic systems PCB in electromagnetic polluted environments," *IEEE Trans. Electromagn. Compat.*, Vol. 59, No. 2, 498-508, 2017.
5. Genender, E., Garbe, H., Sabath, F., "Probabilistic risk analysis technique of intentional electromagnetic interference at system level," *IEEE Trans. Electromagn. Compat.*, Vol. 56, No. 1, 200-207, 2014.
6. Yuhao, C., Kejie, L., Yanzhao, X., "Bayesian assessment method of device-level electromagnetic pulse effect based on Markov Chain Monte Carlo," *APEMC Shenzhen, China, 2016*, 659-661.
7. Jaynes, E. T., "Prior probabilities," *IEEE Trans. Electromagn. Compat.*, Vol. 4, No. 3, 227-241, 1968.
8. Syversveen, A. R., "Non informative Bayesian Priors. interpretation and problems with construction and applications," *Preprint Statistics*, Vol. 3, No. 3, 1-11, 1998.
9. Zellner, A., "Maximal data information prior distributions," *New developments in the applications of Bayesian methods*, 211-232, 1977.
10. Jeffrey, H., "An invariant form for the prior probability in estimation problems," *The Royal Society*, 1947.
11. Berger, J., Bernardo, J., "On the development of the reference prior method," *Bayesian Statistics*, Vol. 4, No. 4, 35-60, 1992.
12. Yang, R., Berger, J. O., *A catalog of noninformative Priors*, Institute of Statistics and Decision Sciences, Duke University, 1996.
13. G. Casella, and R. L. Berger, *Point estimation*, 2nd ed., Pacific Grove, CA: Duxbury, 2002.
14. Ruch, J.J, *Statistique: Estimation. Préparation l'Agrégation Bordeaux*, 11, 2013.
15. Perreault, L., Bobée, B., *Loi Weibull à deux paramètres propriétés mathématiques et statistiques estimation des paramètres et des quantiles X_t de période de retour T* , Sainte-Foy, Quebec, 2002.
16. Hirose, H., "Bias correction for the maximum likelihood estimates in the two-parameter weibull Distribution," *IEEE Trans. Dielectr. Electr. Insul.*, Vol. 6, No. 1, 66-68, 1999.
17. Houret, T., Besnier, P., Vauchamp, S., Pouliguen, P., "Inferring the probability distribution of the electromagnetic susceptibility of equipment from a limited set of data," *EMC Europe, Amsterdam 2018*.
18. Pouant, C., *Caractérisation de la susceptibilité électromagnétique des étages d'entrée de composants électroniques*, PhD. dissertation, Montpellier, France, 103 163–168 2015.